Provided for non-commercial research and education use.
Not for reproduction, distribution or commercial use.

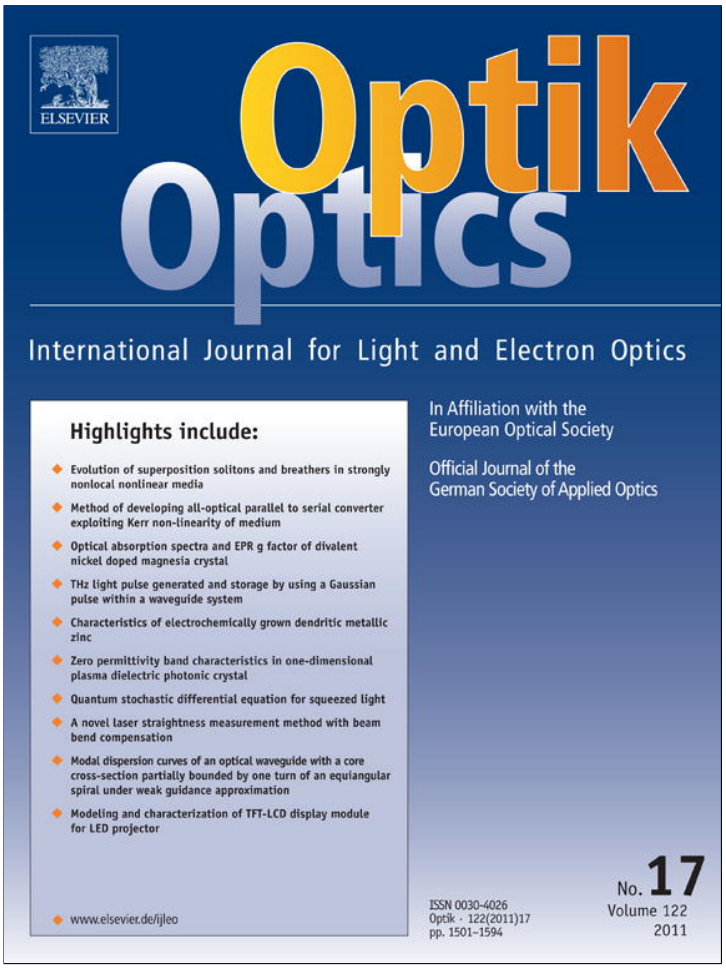

This article appeared in a journal published by Elsevier. The attached copy is furnished to the author for internal non-commercial research and education use, including for instruction at the authors institution and sharing with colleagues.

Other uses, including reproduction and distribution, or selling or licensing copies, or posting to personal, institutional or third party websites are prohibited.

In most cases authors are permitted to post their version of the article (e.g. in Word or Tex form) to their personal website or institutional repository. Authors requiring further information regarding Elsevier's archiving and manuscript policies are encouraged to visit:

http://www.elsevier.com/copyright

Author's personal copy

Optik 122 (2011) 1552–1557

Contents lists available at ScienceDirect

Optik

journal homepage: www.elsevier.de/ijleo

Determination of depth-of-focus in lensless in-line digital particle holography

Yan Yang [a,b], Bo-seon Kang [b,*]

[a] Key Laboratory of Automobile Parts and Test Technique, Ministry of Education, Chongqing University of Technology, 400050, China
[b] Department of Mechanical Systems Engineering, Chonnam National University, Gwangju 500-757, Republic of Korea

ARTICLE INFO

Article history:
Received 6 October 2009
Accepted 25 May 2010

Keywords:
Depth of focus
Digital particle holography
Simulation holograms

ABSTRACT

Lensless in-line digital particle holography (DPH) can be thought of as a special case of photography, and its depth of focus (DoF) characteristics combine those of both photography and holography. The effect of important parameters such as the pixel size and the number of pixels in a charge-coupled device (CCD), the object's distance, the wavelength of the laser, and the particle diameter on the DoF of a reconstruction image in lensless in-line DPH was investigated using simulation holograms. The DoF is directly proportional to the object distance and the particle size. As the wavelength of the laser increases, the DoF decreases. The DoF is inversely proportional to the pixel size and to the number of pixels in a CCD. Instead of expressing nonspecific proportional relationships for DoF, the DoF prediction equations for typical CCD cameras were obtained using DoF data from many simulation holograms and efficient data-fitting software. Finally, the DoF prediction equations were verified using real holograms from a calibration target for several cases. Good agreement between measured and predicted values was confirmed.

© 2010 Elsevier GmbH. All rights reserved.

1. Introduction

Digital particle holography (DPH) is a powerful tool for particle field measurements. It can capture volumetric information of measurement fields instantaneously. Due to the rapid development of charge-coupled device (CCD) cameras and computer technologies, the quality of holograms has improved and the computing speed of image reconstruction has increased. Thus, DPH has strong potential for measuring the features of particles. In recent decades, DPH has been adopted for various particle field measurement applications such as holographic microscopy [1], holographic tomography [2], phase contrast imaging [3], microgravity research [4], and common flow field diagnostics [5–7]. Digital holography is classified as in-line or off-axis depending on the optical set-up. In-line digital holography is widely used because it has a simple optical configuration.

Depth of focus (DoF) indicates the tolerance for the placement of an image plane (a film) within a camera. The DoF is a very important parameter which presents the longitudinal resolution; i.e., the longitudinal range of positions at which an object can be sharply imaged using an imaging module [8–14]. In motion picture cameras, different lens mounts and camera gate combinations have exact flange focal depth measurements to which lenses are calibrated. A well-known principle of DoF in photography is that DoF is proportional to the object's distance and inversely proportional to the aperture. For a lensless optics system, images with infinite DoF can be captured by a pinhole camera instead of using a lens [15]. In this case, the DoF is related to wavelength. For both lensed and lensless systems of photography, exact formulas for DoF are well-known.

DoF is also one of the most important parameters in DPH, and determination of its value affects the precision of particle position extraction. The major differences between photography and holography are as follows. A photographic image is a single unchangeable viewpoint in which the third dimension (depth) is collapsed onto the plane of the detection. Holography does not record an image in the same way a camera does – it captures three complete dimensions of a scene, including its depth. The DoFs in photography and holography are the placement tolerance of a film within a camera and the placement tolerance of a reconstruction image distance, respectively. The light source required in holography must be monochromatic and coherent. Thus, the formula for DoF in photography cannot be used in holography. In optical holography, the DoF depends on particle diameter D_d and the wavelength of the laser, given by $\tau \sim D_d^2/\lambda$ [16]. A similar expression of DoF which only includes the wavelength and the numerical aperture of holograms was presented in [17]. In digital holography using a special filter, the influencing parameters of the DoF were changed to the pixel size of a CCD, Δ, and the wavelength of laser. Thus, $\tau \sim \Delta^2/\lambda$ [18], which gives an effective reduction of DoF when using a special filter. However, the preceding equations only show nonspecific proportional relationships; there is no exact formula for DoF in DPH. The reason

* Corresponding author. Tel.: +82 62 5301683; fax: +82 62 5301689.
E-mail address: bskang@chonnam.ac.kr (B.-s. Kang).

0030-4026/$ – see front matter © 2010 Elsevier GmbH. All rights reserved.
doi:10.1016/j.ijleo.2010.05.038

Author's personal copy

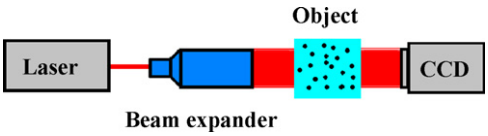

Fig. 1. Optical setup of lensless in-line digital holography.

is that clear theoretical analysis of the parameters determining the depth of focus is difficult to obtain in mathematics.

In this study, the effect of all influencing parameters such as the pixel size and number of pixels in a CCD, the object distance, the wavelength of the laser, and the particle diameter on the DoF in lensless in-line DPH was evaluated using simulation holograms. The change in DoF with different parameter values was investigated, and the DoF prediction equations for typical CCD cameras are presented. A calibration target was used to verify the correctness of the equations, and good agreement was obtained.

2. General principles

Hologram recording and object reconstruction is similar to that of optical holography. However, digital holography has several obvious advantages over optical holography. The recording medium is a CCD digital image instead of photographic film. The reconstruction of recorded holograms is performed by a computer, which is called numerical reconstruction. Digital holography is either lensless or uses a lens. Lensless digital holography is widely used because it has a simple optical configuration and high precision.

The concept of lensless in-line digital holography is shown in Fig. 1. An expanded laser beam goes through the object field. The part of beam diffracted by objects and arriving at the recording surface is the object beam, and the beam arriving without distortion by objects is the reference beam. The superposition of the two beams creates an interference pattern on the CCD sensor. This diffraction can be described by the Fresnel–Kirchhoff integral [19]:

$$R(\xi', \eta') = \frac{i}{\lambda}\int_{-\infty}^{\infty}\int_{-\infty}^{\infty} h(x,y)E_R(x,y)\frac{\exp(-i2\pi/\lambda\rho)}{\rho}dxdy \quad (1)$$

with

$$\rho = \sqrt{(\xi' - x)^2 + (\eta' - y)^2 + d^2} \quad (2)$$

The coordinates of Eqs. (1) and (2) are shown in Fig. 2. $R(\xi', \eta')$, $h(x, y)$, and $E_R(x, y)$ are functions of the reconstruction image, hologram, and reference, respectively. Here, d is the distance between two adjacent planes, λ is the wavelength, and ρ is the distance between two corresponding points in two adjacent planes.

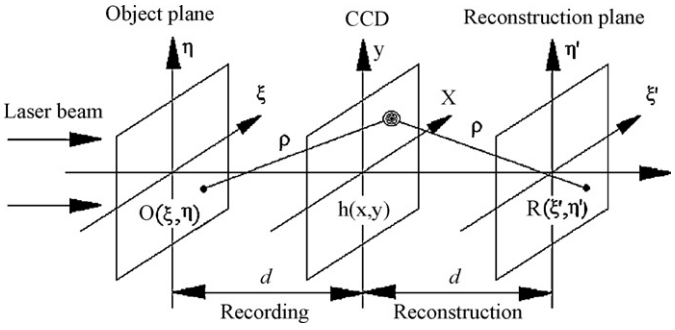

Fig. 2. Coordinate system of recording and reconstruction in digital holography.

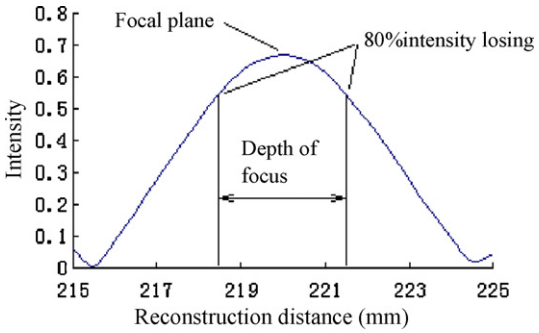

Fig. 3. Determination of DoF (particle diameter is 7.4 μm, object distance is 220 mm).

The reconstruction image, $R(\xi', \eta')$, can be obtained by the Fresnel method or the convolution method [19]. In our previous study [20], the resolution of the reconstruction image by the convolution method was better than the image from the Fresnel method. Therefore, the convolution method was used in the present study. The mathematical expression of the convolution method is

$$R(\xi', \eta') = F^{-1}\left\{F[h(x,y)]\cdot F\left[\frac{i}{\lambda}\frac{\exp[-i(2\pi/\lambda)\sqrt{(d^2+(x-\xi')^2+(y-\eta')^2}]}{\sqrt{(d^2+(x-\xi')^2+(y-\eta')^2}}\right]\right\} \quad (3)$$

where F and F^{-1} are the Fourier transform and its inverse, respectively.

Based on the theory of Fresnel holography, the minimum object distance in Fresnel holography is given by

$$d \geq \sqrt[3]{\frac{1}{8}\frac{[(\xi - x)^2 + (\eta - y)^2]^2_{\max}}{\lambda}} \quad (4)$$

where the coordinates are shown in Fig. 2 [19]. When the numerator is chosen to be the maximum, the object must be at the origin in the object plane, and the CCD is filled with the interference pattern of the object. These mean that ξ and η are zero, and the maximum coordinates of x and y occur at the corner in the hologram plane. In Eq. (4), the value of minimum distance increases with the size of CCD. In this work, the maximum size of the CCD is 2048 pixels × 7.4 μm, and the wavelength λ is 632.8 nm (for a He–Ne laser) or 532 nm (for an Nd–YAG laser). Thus, the minimum object distances in these cases are $d \geq 137.59$ mm for a He–Ne laser and $d \geq 145.79$ mm for an Nd–YAG laser. Thus, all object distances in the holograms discussed in the present study are greater than these minimum distances.

3. Parametric analysis

In holography, the definition of the DoF of a reconstruction image can be taken as an interval around the focal plane such that the intensity of the reconstruction image decreases more than 20%. A typical intensity distribution of a reconstruction image and the resulting determination of its DoF are shown in Fig. 3.

In this section, simulation holograms generated by the convolution method are used to evaluate the important parameters of the DoF in lensless in-line DPH [21]. We reconstructed a simulation hologram around the focal plane and obtained the value of the corresponding DoF based on the preceding definition. DoFs from many simulation holograms under several different conditions were calculated automatically using a processing program, and the trend of the DoF for different parameter values was examined. Using these results, the effects of important parameters used in digital hologram reconstruction on the DoF were investigated. The relationships between these parameters and the DoF are described as follows.

Author's personal copy

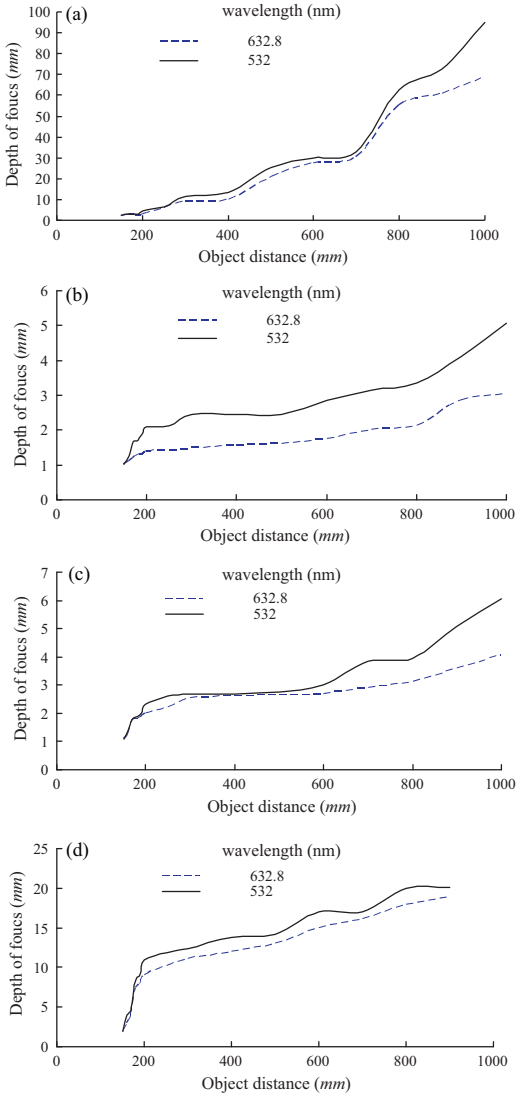

Fig. 4. Effect of wavelength of laser on DoF.

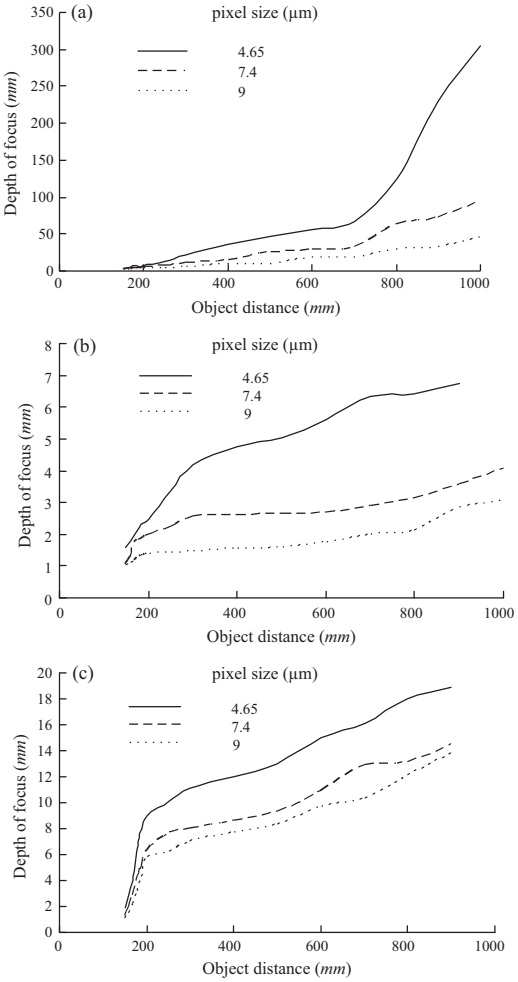

Fig. 5. Effect of pixel size on DoF.

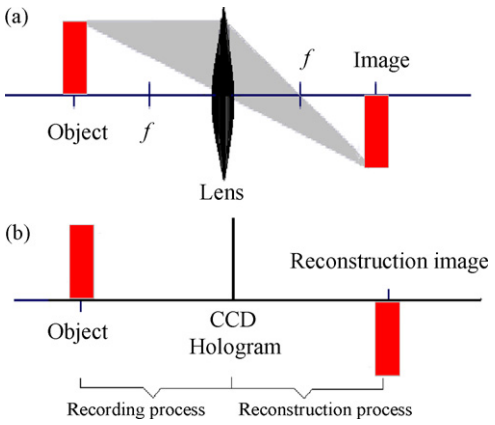

Fig. 6. Comparison of imaging processes between photographic imaging and lensless in-line digital holography.

3.1. Wavelength λ

Lasers used to generate digital particle holograms are typically Nd–Yag lasers or He–Ne lasers. Therefore, we examined DoF using the wavelengths of these lasers. Our results revealed that DoF is inversely proportional to laser wavelength regardless of pixel size Δx, the pixel numbers N, the particle diameter D_d, and the object distance d. The relationship between the DoF and the wavelength of the laser in digital holography is consistent with the approximate expression in optical holography [16]. These results are shown in Fig. 4.

3.2. Pixel size

Pixel size; i.e., the resolution of a hologram, is an important parameter influencing the reconstruction image. In digital holography, the pixel sizes of common CCD cameras are 4.65, 7, and 9 μm. Thus, we checked the DoFs corresponding to these values using simulation holograms under different conditions. The typical results, shown in Fig. 5, revealed that DoF is inversely proportional to the pixel size of a CCD camera. This relationship is opposite to that of the DoF formula presented in other literatures which involve optics systems using a lens or special filters [18,23,24]. In this study, the holographic system is conventional lensless digital holography, which has no lens between the object and the CCD. Therefore, when we reconstruct images, we do not use filters or a magnification factor.

Because the reconstruction image in the focal plane has the same size as the object, the reconstruction process of a lensless digital hologram in the focal plane is a special case of the optical imaging system using a lens as shown in Fig. 6. To obtain the same size of image as the object in an imaging system using a lens, the lens must

Author's personal copy

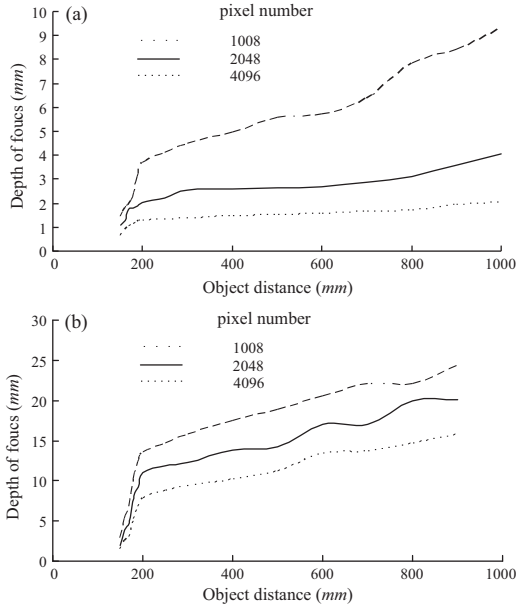

Fig. 7. Effect of pixel number on DoF.

be placed in the middle of the object and the image plane. The distance from the lens to the image plane is twice the focal length of the lens, as shown in Fig. 6(a). When the parameter settings are as previously described, the DoF is also inversely proportional to the pixel size as a special case of the DoF calculation for a digital camera [23]. The recording and reconstruction processes of a lensless digital hologram in the focal plane must be similar to the processes in Fig. 6(a). As shown in Fig. 6(b), the CCD camera (hologram) can be regarded as a lens in the photographic system in Fig. 6(a). In addition, when the pixel size decreases, the numerical aperture decreases with the fixed pixel number, so the DoF increases. Therefore, the DoF is inversely proportional to the pixel size of the CCD camera in lensless in-line DPH.

3.3. Pixel number

We now consider the influence of the pixel number of a CCD camera on DoF. The pixel numbers of simulation holograms were chosen as 1008, 2048, and 4096 based on common CCD cameras. Typical results are shown in Fig. 7. The results showed that the pixel number has a strong effect on the DoF, which is directly proportional to the pixel number. The reason is that an increase in pixel number is equal to the increase in aperture in optical photography. When the aperture becomes larger, the DoF becomes smaller. This relationship was also verified in optical holography and digital holography (numerical aperture) [15,17]. Therefore, DoF decreases with an increase in the pixel number in lensless in-line digital holography.

3.4. Particle diameter

Vikram suggested that DoF is directly proportional to particle diameter [16], which was also mentioned in our previous research [22]. The effect of particle diameter on DoF is shown in Fig. 8 for $\lambda = 632.8$ nm, $\Delta x = 7.4$ μm, and $N = 1008$. The DoF is directly proportional to the particle diameter.

3.5. Object distance

The quality of reconstruction images in digital holography becomes poor as the object distance increases [20]. When we

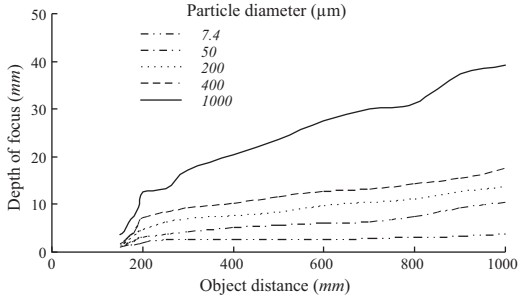

Fig. 8. Effect of particle diameter on DoF.

reconstruct a hologram which is generated by a far object, the reconstruction image, even at the focal plane, is unclear. This means the reconstruction image at the focal plane is almost similar to the images at the defocal planes. Thus, when the object is far from the CCD, the reconstruction image in lensless in-line digital holography has a longer DoF than is the case when the object is close to the CCD; i.e., DoF is directly proportional to the object distance. This trend can be observed in Figs. 4–8, and is in agreement with the theory of common optics.

4. Prediction equations

We produced prediction equations for DoF in typical cases by a data fitting method. Based on the specifications of common cameras used in digital holography, typical values of the important parameters are as follows: The pixel numbers of common CCD cameras are 1008×1018 and 2048×2048, and the pixel sizes are 9 and 7.4 μm. The pixel numbers of holograms generated by these cameras are 1008×1008 and 2048×2048, respectively. The wavelengths of commonly used lasers are 632.8 nm and 532 nm. After obtaining extensive data for DoF in lensless in-line DPH using simulation holograms, TableCurve 3D V4.0 (SYSTAT Software Inc.) software was used to acquire fitting surfaces and prediction equations. TableCurve 3D combines a powerful surface fitter with the ability to find the ideal equation to describe three dimensional empirical data.

4.1. Case of $N = 1008$, $\Delta x = 9\,\mu m$

DoFs at different particle diameters with different object distances were calculated. The calculation interval of the object distance was from 100 to 1000 mm, which was based on the requirement of actual measurements. The increment of the object distance was 20 mm considering the precision and the calculation speed. We specified the particle diameter as a function of the pixel size:

$$D_d = (2n-1)\Delta x, \quad n = 1, 2, \ldots, M. \tag{5}$$

M was chosen as 57 because the maximum particle diameter in a practical measurement is usually less than 1000 μm. After calculating DoFs for every case, 2622 data elements showing the variation in DoF were obtained. Using the software, the fitting surface and the equation of the DoF were obtained. The best fitting surfaces of the DoFs are shown in Fig. 9. The goodness-of-fit value r^2 (the fit standard error in Fig. 9(a) and (b)) are 0.99096986 and 0.99254606, respectively.

The mathematical forms of the prediction equations of DoF τ at each laser wavelength are as follows:

$$\tau = \frac{a + b\ln d + c(\ln d)^2 + k(\ln d)^3 + e\ln D_d + f(\ln D_d)^2}{1 + g\ln d + h\ln D_d + i(\ln D_d)^2 + j(\ln D_d)^3} \tag{6}$$

Author's personal copy

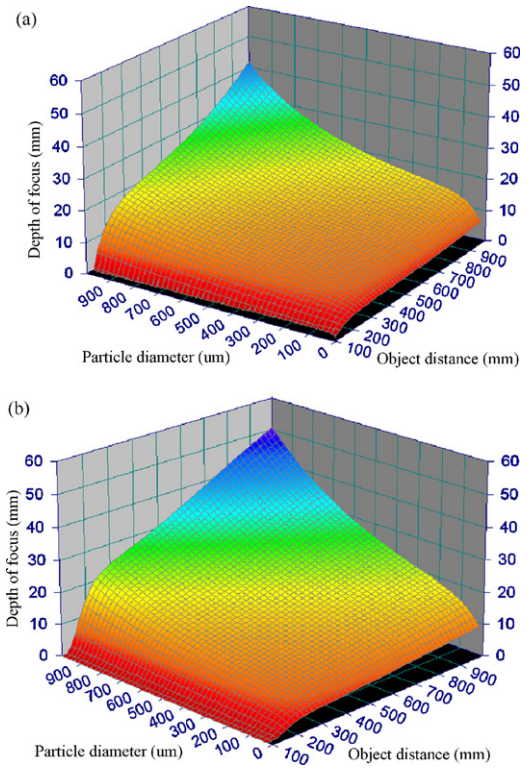

Fig. 9. Fitting surface of DoF for the case of $N = 1008$, $\Delta x = 9\ \mu m$: (a) $\lambda = 632.8$ nm, and (b) $\lambda = 532$ nm.

at $\lambda = 632.8$ nm,

$$\tau = \exp\left(a + \frac{b}{\sqrt{d}} + \frac{c\ln d}{d} + \frac{k}{d} + \frac{e}{d^{3/2}} + f\sqrt{D_d}\ln D_d + \frac{gD_d}{\ln D_d} + h\sqrt{D_d}\right) \quad (7)$$

at $\lambda = 532$ nm.

The coefficients a–k in Eqs. (6) and (7) are shown in Table 1. The conditions of Eqs. (6) and (7) are the pixel size $\Delta x = 9\ \mu m$ and the pixel number $N = 1008$. These equations can be used to determine the DoFs for the Roper Scientific Megaplus ES 1.0 CCD camera or the Kodak ES 1.0 CCD camera.

4.2. Case of $N = 2048$, $\Delta x = 7.4\ \mu m$

The DoFs for the case of $N = 2048$, $\Delta x = 7.4\ \mu m$ were calculated. For this case, $M = 68$ and 3128 data elements were collected. Based on these data, the best fitting surfaces of DoFs are shown in Fig. 10. The goodness-of-fit value r^2 in Fig. 10(a) and (b) is 0.98613826 and 0.98019215, respectively.

The DoF prediction equation τ at each laser wavelength is

$$\tau = a + b\ln d + cD_d + k(\ln d)^2 + eD_d^2 + fD_d\ln d + g(\ln d)^3 + hD_d^3 + iD_d^2\ln d + jD_d(\ln d)^2 \quad (8)$$

at $\lambda = 632.8$ nm and 532 nm with different coefficients, as shown in Table 1.

The DoF for the Roper Scientific Megaplus 4.0 CCD camera or the Redlake Megaplus II ES4020 CCD camera can be determined using this equation.

5. Validation experiments

To verify the correctness of the prediction equations for DoFs described in the previous section, a calibration target with various sizes of dots ranging from 8 to 300 μm was used as shown in Fig. 11.

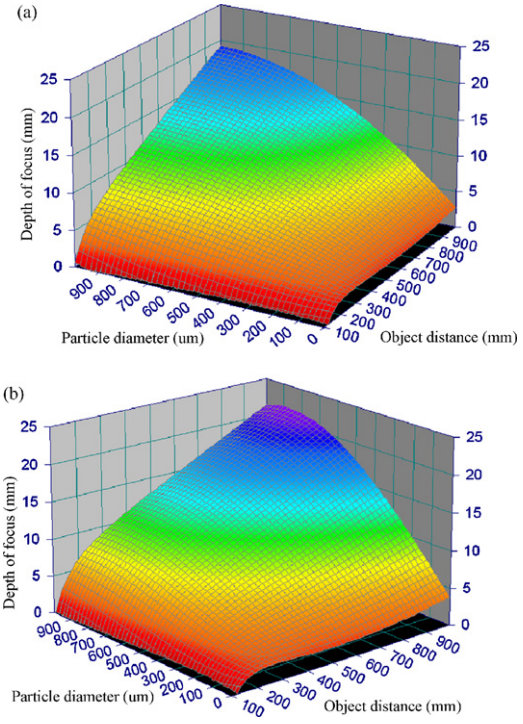

Fig. 10. Fitting surface of DoF for the case of $N = 2048$, $\Delta x = 7.4\ \mu m$: (a) $\lambda = 632.8$ nm, and (b) $\lambda = 532$ nm.

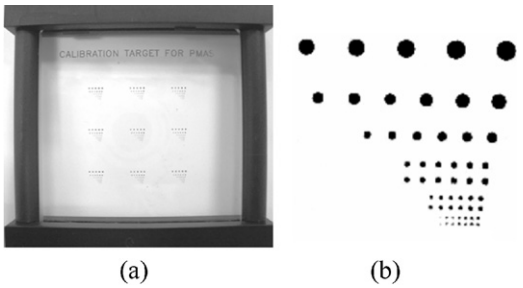

Fig. 11. Calibration target with different size particles: (a) calibration target and (b) magnified image of different sizes of dots.

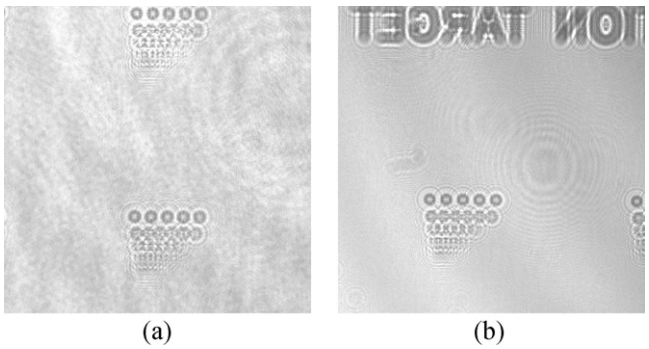

Fig. 12. Holograms of calibration target.

The holograms were taken by a typical CCD camera, the Redlake Megaplus II ES4020, whose pixel size and number are 7.4 μm and 2048 × 2048, respectively. The holograms of the calibration target generated by different lasers are shown in Fig. 12.

Using the correlation coefficient method [22], the calculated focal planes of each hologram are 240.05 and 210.36 mm, respectively. Based on these values of the focal planes, we reconstructed

Author's personal copy

Table 1
Coefficients from Eqs. (6)–(8).

	Eq. (6) λ = 632.8 nm	Eq. (7) λ = 532 nm	Eq. (8) λ = 632.8 nm	Eq. (8) λ = 532 nm
a	−63.928623	−4.6331195	−325.48841	−437.2604
b	32.181276	976.08605	164.20855	224.64208
c	−5.3075527	−12,932.301	−0.006504813	−0.057321606
e	0.33872165	−204,600.58	5.7500632e−5	8.7182136e−5
f	0.033483965	−0.13339165	−0.011180253	0.0021926936
g	−0.0073906396	0.077429683	1.5158471	2.155625
h	−0.47480124	0.67925082	−7.120578e−10	−1.282086e−8
i	0.084559688		−1.0399222e−5	−1.2817773e−5
j	−0.0051103452		0.0024151199	0.0015502325
k	0.29259601	69942.467	−27.3644	−38.168489

Table 2
Comparison between measured values and predicted values for DoF.

	DoF (*mm*) Particle diameter (μm)				
	10	51	100	230	300
λ = 532 nm					
Measured values	2.319	2.413	2.603	3.355	3.869
Predicted values	2.322	2.414	2.591	3.338	3.864
Errors (μm)	3	1	12	17	5
λ = 632.8 nm					
Measured values	1.940	2.064	2.216	2.655	2.920
Predicted values	1.938	2.057	2.207	2.643	2.897
Errors (μm)	2	7	9	12	23

the holograms slice-by-slice along the optical axis using the reconstruction interval, and obtained the DoF for different sizes of particles. A comparison between the measured values and the predicted values calculated using Eq. (8) is shown in Table 2.

In these results, the maximum error was 23 μm (0.7% of predicted value), and the mean errors for λ = 532 nm and λ = 632.8 nm were 7.6 μm and 10.6 μm, respectively. In this study, the measurement precision; i.e., the reconstruction interval, was 1 μm, and the goodness-of-fit values were over 99%. Thus, errors existing in the experimental measurements and the data fitting had no significant effect on the comparison results. Thus, the errors are acceptable, which proves that the prediction equations can work well for the determination of DoF.

6. Conclusions

Using simulation holograms, important parameters influencing the DoF in lensless in-line DPH such as the pixel size and number of the CCD, the object distance, the wavelength of the laser, and the particle diameter were discussed. Lensless in-line DPH can be thought of as a special case of photography based on its properties, with characteristics existing in both photography and holography. Depth-of-focus is directly proportional to the object distance and the particle size, and is inversely proportional to the wavelength of the laser, and to the pixel size and number of the CCD. The exact prediction equations of the DoF for two typical CCD cameras were obtained using data fitting software. The goodness-of-data-fitting was over 99%. Finally, the equations for DoF in lensless in-line DPH were verified by investigating real holograms of the calibration target for different cases, and good agreements were obtained.

Acknowledgement

This work was supported by the Korea Research Foundation Grant funded by the Korean Government (KRF-2008-313-D00137), by the Natural Science Foundation Project of CQ CSTS (2010BB2087), and by the Priming Scientific Research Foundation of CQUT(2009zd29).

References

[1] F. Palacios, J. Ricardo, D. Palacios, E. Gonçalves, J.L. Valin, R.D. Souzac, 3D image reconstruction of transparent microscopic objects using digital holography, Opt. Commun. 248 (2005) 41–50.
[2] M.K. Kim, Tomographic three-dimensional imaging of a biological specimen using wavelength-scanning digital interference holography, Opt. Exp. 7 (2000) 305–310.
[3] F. Bevilacqua, C. Depeursinge, Digital holography for quantitative phase-contrast imaging, Opt. Lett. 24 (1999) 291–293.
[4] R.B. Owen, A.A. Zozulya, M.R. Benoit, D.M. Klaus, Microgravity materials and life sciences research applications of digital holography, Appl. Opt. 41 (2002) 3927–3935.
[5] G. Pan, H. Meng, Digital in-line holographic PIV for 3D particulate flow diagnostics, in: Proceeding of 4th International Symposium on PIV, 2001, pp. 1–5.
[6] H. Meng, G. Pan, Y. Pu, S.H. Woodward, Holographic particle image velocimetry: from film to digital recording, Meas. Sci. Technol. 15 (2004) 673–685.
[7] M. Malek, D. Allano, S. Cöetmellec, C. Ozkul, D. Lebrun, Digital in-line holography for three dimensional-two-components particle tracking velocimetry, Meas. Sci. Technol. 15 (2004) 699–705.
[8] E. Dowski, W.T. Cathey, Extended depth of field through wave-front coding, Appl. Opt. 34 (1995) 1859–1866.
[9] J.V.D. Gracht, E. Dowski, M. Taylor, D. Deaver, Broadband behavior of an optical-digital focus-invariant system, Opt. Lett. 21 (1996) 919–921.
[10] J.O. Castaneda, E. Tepichin, A. Diaz, Arbitrarily high focal depth with a quasi-optimum real and positive transmittance apodizer, Appl. Opt. 28 (1989) 2666–2670.
[11] E.B. Eliezer, Z. Zalevsky, E. Marom, N. Konforti, All-optical extended depth of field imaging system, J. Opt. A: Pure Appl. Opt. 5 (2003) S164–S169.
[12] Z. Zalevsky, A. Shemer, A. Zlotnik, E.B. Eliezer, E. Marom, All-optical axial super resolving imaging using a low-frequency binary-phase mask, Opt. Exp. 14 (2006) 2631–2643.
[13] A. Sauceda, J.O. Castañeda, High focal depth with fractional-power wavefronts, Opt. Lett. 29 (2004) 560–562.
[14] Z. Zalevsky, J. Garcı′a, All-optical super resolved and extended depth of focus imaging with random pinhole array aperture, Opt. Commun. 281 (2008) 953–957.
[15] J.W. Goodman, Introduction to Fourier Optics, McGraw-Hill, USA, 1996.
[16] C.S. Vikram, Particle Field Holography, Cambridge University Press, UK, 1992.
[17] H. Meng, F. Hussain, IROV (In-Line Recording and Off-Axis Viewing) technique for holographic particle velocimetry, Appl. Opt. 34 (2004) 1827–1840.
[18] W.D. Yang, A.B. Kostinski, R.A. Shaw, Reduction for digital in-line holography of particle fields, Opt. Lett. 30 (2005) 1303–1305.
[19] U. Schnars, W. Jueptner, Digital Holography, Springer, New York, 2005.
[20] Y. Yang, B.S. Kang, Application of digital holography to sprays, in: Proceedings of Asia Display, 2007, pp. 2050–2054.
[21] Y. Yang, B.S. Kang, Numerical simulation of in-line digital holograms, in: Proceedings of Asia Display, 2007, pp. 2055–2059.
[22] Y. Yang, B.S. Kang, Y.J. Choo, Application of the correlation coefficient method for determination of the focal plane to digital particle holography, Appl. Opt. 47 (2008) 817–824.
[23] Calculate depth of focus for digital cameras, copyright Lindolfi. www.kalons.nl/otten/DoFdigitalEng.html.
[24] M.C. Raúl, S. Genaro, M.C. Manuel, J. Bahram, Enhanced depth of field integral imaging with sensor resolution constraints, Opt. Exp. 12 (2004) 5237–5243.